Wind and Structures, Vol. 13, No. 3 (2010) 235-256
DOI: http://dx.doi.org/10.12989/was.2010.13.3.235

Prevention of suspension bridge flutter using multiple tuned mass dampers

Filippo Ubertini*

Department of Civil and Environmental Engineering,
University of Perugia, Via G. Duranti 93, 06125 Perugia, Italy

(Received January 16, 2009, Accepted October 20, 2009)

Abstract. The aeroelastic stability of bridge decks equipped with multiple tuned mass dampers is studied. The problem is attacked in the time domain, by representing self-excited loads with the aid of aerodynamic indicial functions approximated by truncated series of exponential filters. This approach allows to reduce the aeroelastic stability analysis in the form of a direct eigenvalue problem, by introducing an additional state variable for each exponential term adopted in the approximation of indicial functions. A general probabilistic framework for the optimal robust design of multiple tuned mass dampers is proposed, in which all possible sources of uncertainties can be accounted for. For the purposes of this study, the method is also simplified in a form which requires a lower computational effort and it is then applied to a general case study in order to analyze the control effectiveness of regular and irregular multiple tuned mass dampers. A special care is devoted to mistuning effects caused by random variations of the target frequency. Regular multiple tuned mass dampers are seen to improve both control effectiveness and robustness with respect to single tuned mass dampers. However, those devices exhibit an asymmetric behavior with respect to frequency mistuning, which may weaken their feasibility for technical applications. In order to overcome this drawback, an irregular multiple tuned mass damper is conceived which is based on unequal mass distribution. The optimal design of this device is finally pursued via a full domain search, which evidences a remarkable robustness against frequency mistuning, in the sense of the simplified design approach.

Keywords: deck flutter; indicial functions; Hopf bifurcation; multiple tuned mass dampers; frequency mistuning; robust control.

1. Introduction

Long-span suspension bridges are lightly damped structures where wind loads may produce large amplitude oscillations or even catastrophic instability. Thus, increasing the safety against aeroelastic instability is mandatory in bridge engineering.

Mechanically speaking, the flutter instability of a bridge deck section ensues from a Hopf bifurcation which leads to unstable coupled bending-torsional motions (Piccardo 1993, Simiu and Scanlan 1996, Chen, *et al.* 2000a). The aeroelastic stability analysis requires therefore self-excited loads to be modeled. To this end, either frequency domain (Robertson, *et al.* 2003) or time domain (Chen, *et al.* 2000b, Lazzari, *et al.* 2004) formulations can be adopted. Likewise in response

* Corresponding Author, Assistant Professor, E-mail: filippo.ubertini@strutture.unipg.it

problems (Gusella and Materazzi 2000, Cluni, *et al.* 2007, Tubino and Solari 2007), time domain formulations have the advantage of easily handling the presence of structural nonlinearities. The most effective and up-to-date method to express aeroelastic forces for bridge deck sections in the time domain, is probably represented by the load model using indicial functions (Scanlan, *et al.* 1974, Costa and Borri 2006, Salvatori and Borri 2007). This model was formulated directly in the time domain for the thin airfoil. Its extension to bluff cross-sections is due to Scanlan, *et al.* (1974) and it is based on the exponential approximation of Wagner's function. Practically, indicial functions are often approximated via truncated series of exponential filters and the unknown parameters are identified from measured aeroelastic derivatives via optimization procedures (Costa and Borri 2006). Though slightly approximated, this simple approach is very popular because well-established experimental techniques currently exist only for the determination of the aeroelastic derivatives. Nonetheless, it must be mentioned that some promising studies for a direct experimental assessment of indicial functions were already proposed by some researchers (Caracoglia and Jones 2003).

Structural control is nowadays a well-established field in the technical literature (Soong 1991, Breccolotti, *et al.* 2007, Casciati, *et al.* 2007, Ubertini 2008a, Faravelli, *et al.* 2009, Faravelli and Ubertini 2009) and it is commonly accepted as a key point of modern structural design. Within this topic, a great attention was recently devoted to conceiving control strategies against bridge flutter. On this respect, many studies were focused on the use of single and multiple tuned mass dampers (Gu, *et al.* 1998, Lin, *et al.* 1999, 2000, Pourzeynali and Datta 2002, Kwon 2002, Chen and Kareem 2003, Kwon and Park 2004, Ubertini 2008b), although active control solution were also investigated (Preidikman and Mook 1997, Kwon and Chang 2000). Single tuned mass dampers (STMDs) are especially prone to mistuning effects (see for instance, Lin, *et al.* (2000)). This circumstance, in the case of the classic coupled flutter instability of a bridge deck, makes the STMD solution practically unfeasible. Indeed, in such a case, the calculation of the optimal tuning of the device, close to the critical frequency of the system, is affected by aerodynamic and structural uncertainties and mistuning is basically unpreventable. Multiple tuned mass dampers (MTMDs), with equal amount of mass with respect to the STMDs, are known to enhance the control robustness in presence of mistuning effects (see for instance, Kwon and Park (2004)). These devices are composed by several small tuned mass dampers (TMDs) whose natural frequencies are equally spaced around a mean value which corresponds to the frequency that has to be controlled (Abe and Fujino 1994, Kareem and Kline 1995). The concept of irregular multiple tuned mass dampers (IMTMDs) for deck flutter control was also proposed by Kwon and Park (2004). These devices are obtained by irregularly distributing either the natural frequencies or the damping ratios of the small TMDs. Such an approach allows to obtain enhanced control effectiveness with respect to the regular MTMD case (Kwon and Park 2004). However, despite the rich technical literature devoted to the topic, some aspects about the use of regular and irregular MTMDs still deserve further investigations. Indeed, these control devices significantly enhance the complexity of the system and the optimization of the control parameters may become a very difficult task, especially when IMTMDs are concerned (Kwon and Park 2004). Therefore, a complete understanding of all the involved aspects related to the aeroelastic stability of deck-MTMDs systems is still missing.

The paper presents an investigation on the use of regular and irregular MTMDs to increase the critical velocity leading to bridge flutter. Due to the large number of degrees of freedom of the considered mechanical system, applying the classic iterative search of the Hopf bifurcation point in the frequency domain (Simiu and Scanlan 1996, Robertson, *et al.* 2003) becomes especially troublesome. Therefore, the aeroelastic stability analysis is performed in the time domain, via a direct eigenvalue

problem, by representing the aeroelastic loads through indicial functions. A general technique for the optimal robust design of MTMDs is then presented, which makes use of a probabilistic measure of control effectiveness and it is based on a level 1 reliability analysis. The method, which allows to fully consider the role played by all kind of uncertainties affecting the system, is then simplified in a less computationally expensive form and applied to a general case study. The results show that a correct design of the regular MTMD may enlarge the frequency band of control effectiveness with respect to the STMD. However, some asymmetry in the behavior of the system with respect to frequency mistuning is evidenced, which partially reduces the feasibility of the device for technical applications. After giving an interpretation of this phenomenon, an IMTMD with irregular mass distribution is proposed to circumvent this drawback. Once the configuration of the IMTMD offering the best compromise between control robustness and control effectiveness is found, optimization of damping ratio and frequency tuning of the device is finally performed by means of a full domain search.

2. Governing relations

2.1. Mechanical system

Let us consider the aeroelastic stability of a suspension bridge subjected to an incoming wind flow with mean velocity U and equipped with a MTMD as shown in Fig. 1(a). The aeroelastic lift force per unit length $L(x)$, the pitching moment per unit length $M(x)$, the vertical degree of freedom (DOF) $h(x,t)$ and the twist rotation $\alpha(x,t)$ are defined as shown in Fig. 1(b), x being the longitudinal axis of the deck and t denoting time. The MTMD is obtained by splitting a STMD device (Lin, *et al.* 2000) into n small TMDs of the type shown in Fig. 1(b), with the same total amount of mass of the STMD case. The MTMD is said to be "regular" if the assembled TMDs have same masses, same damping ratios and their natural frequencies are regularly spaced. Otherwise, the MTMD is said to be "irregular".

According to the notation adopted in Fig. 1, the i-th TMD (for i=1,2,...,n), placed at the position x_i, is characterized by: vertical DOF h_{Ti}, rotation α_{Ti}, mass m_{Ti}, mass moment of inertia I_{Ti}, vertical stiffness k_{Ti}, damping coefficient c_{Ti}, vertical damping ratio ξ_{Ti}, torsional damping ratio $\xi_{T\alpha i}$, vertical

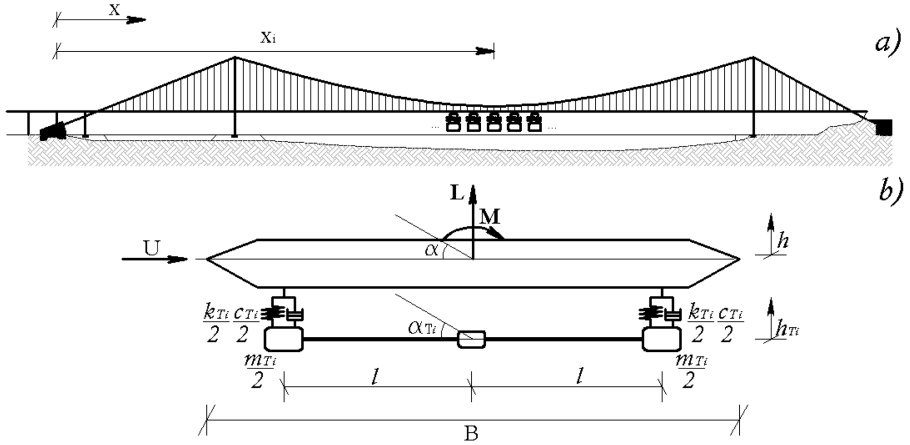

Fig. 1 (a) Sketch of the bridge-MTMD system and (b) i-th TMD device composing the MTMD

natural circular frequency ω_{Ti} and torsional natural circular frequency $\omega_{T\alpha i}$. The reference width of the deck is denoted by $B=2b$, while the half brace of the TMDs is denoted by l.

Clearly, the following relations hold for the considered TMDs (for i=1,2,...,n):

$$\begin{aligned} \omega_{T\alpha i}^{\ 2} &= \omega_{Ti}^{\ 2} \cdot m_{Ti} l^2 / I_{Ti} \\ \xi_{T\alpha i} &= \xi_{Ti} \omega_{T\alpha i} / \omega_{Ti} \end{aligned} \tag{1}$$

The first expression of Eq. (1) indicates that, in general, the vertical and rotational natural frequencies of the i-th TMD are distinct. However, when dealing with the classic flutter instability of bridge decks, it is more convenient to tune the two frequencies to the same value which, in the STMD case, nearly corresponds to the critical flutter circular frequency of the uncontrolled system. This can be achieved by simply concentrating two equal masses at the positions of the elastic and viscous forces, such that, in Eq. (1), it results $I_{Ti}=m_{Ti}l^2$.

As it is well-known, suspension bridge flutter is usually dominated by the first in-plane symmetric and the first torsional symmetric modes. Therefore, for the sake of simplicity, the motion of the bridge is here described by means of these two modes, whose modal shapes are denoted by $\varphi_h(x)$ and $\varphi_\alpha(x)$, respectively. Thus, the vertical and torsional displacement functions can be written as:

$$\begin{aligned} h(x,t) &= \varphi_h(x) \cdot \zeta(t) \\ \alpha(x,t) &= \varphi_\alpha(x) \cdot \gamma(t) \end{aligned} \tag{2}$$

ζ and γ being the modal amplitudes. In the following developments, the vertical and torsional mass ratios of the i-th TMD, with respect to the corresponding generalized modal masses of the bridge $\tilde{m}$ and $\tilde{I}$, are denoted by ψ_i and $\psi_{\alpha i}$, respectively. The aeroelastic stability analysis is then performed by means of a classic two degrees-of-freedom (DOFs) model. In presence of only one STMD (i=n=1), the equations of motion of this simple mechanical system read as (Lin, *et al.* 2000):

$$\begin{aligned} &\tilde{m}[\ddot{\zeta} + (2\xi_h\omega_h + 2\psi_1\xi_{T1}\omega_{T1})\dot{\zeta} + (\omega_h^{\ 2} + \psi_1\omega_{T1}^2)\zeta - 2\psi_1\xi_{T1}\omega_{T1}\dot{\tilde{h}}_T - \psi_1\omega_{T1}^2\tilde{h}_{T1}] = \int_x L(x)\varphi_h(x)dx \\ &\tilde{I}[\ddot{\gamma} + (2\xi_\alpha\omega_\alpha + 2\psi_{\alpha1}\xi_{T\alpha1}\omega_{T\alpha1})\dot{\gamma} + (\omega_\alpha^{\ 2} + \psi_{\alpha1}\omega_{T\alpha1}^2)\gamma - 2\psi_{\alpha1}\xi_{T\alpha1}\omega_{T\alpha1}\dot{\tilde{\alpha}}_{T1} - \psi_{\alpha1}\omega_{T\alpha1}^2\tilde{\alpha}_{T1}] \\ &= \int_x M(x)\varphi_\alpha(x)dx \\ &\ddot{\tilde{h}}_{T1} + 2\xi_{T1}\omega_{T1}(\dot{\tilde{h}}_{T1} - \dot{\zeta}) + \omega_{T1}^2(\tilde{h}_{T1} - \zeta) = 0 \\ &\ddot{\tilde{\alpha}}_{T1} + 2\xi_{T\alpha1}\omega_{T\alpha1}(\dot{\tilde{\alpha}}_{T1} - \dot{\gamma}) + \omega_{T\alpha1}^2(\tilde{\alpha}_{T1} - \gamma) = 0 \end{aligned} \tag{3}$$

where $\tilde{h}_{T1}$ and $\tilde{\alpha}_{T1}$ are the displacements of the STMD in the generalized coordinate system, while the dots denote differentiation with respect to time t. In Eq. (3), ξ_h, ξ_α denote the damping ratios and ω_h, ω_α the natural circular frequencies of the considered bending and torsional modes. The equations of motion of the system for n>1 (MTMD case) can simply be obtained by extending Eq. (3) to the presence of n small TMDs (Kwon and Park 2004).

2.2. Time domain formulation of aeroelastic forces via indicial functions

The aeroelastic forces in Eq. (3) can be expressed through the well-known time domain formulation using indicial functions $\Phi_{Lh}(t)$, $\Phi_{L\alpha}(t)$, $\Phi_{Mh}(t)$ and $\Phi_{M\alpha}(t)$ (Salvatori and Borri 2007), as:

$$\begin{aligned} L &= \frac{1}{2}\rho U^2 B C_L' \left(\Phi_{Lh}(0)\frac{\dot{h}}{U} + \Phi_{L\alpha}(0)\alpha + \int_0^t \dot{\Phi}_{Lh}(t-\tau)\frac{\dot{h}(\tau)}{U}d\tau + \int_0^t \dot{\Phi}_{L\alpha}(t-\tau)\alpha(\tau)d\tau \right) \\ M &= \frac{1}{2}\rho U^2 B^2 C_M' \left(\Phi_{Mh}(0)\frac{\dot{h}}{U} + \Phi_{M\alpha}(0)\alpha + \int_0^t \dot{\Phi}_{Mh}(t-\tau)\frac{\dot{h}(\tau)}{U}d\tau + \int_0^t \dot{\Phi}_{M\alpha}(t-\tau)\alpha(\tau)d\tau \right) \end{aligned} \tag{4}$$

where ρ denotes the air density while C_L' and C_M' are the so-called "dynamic derivatives". These lasts represent the derivatives of the aerodynamic lift and moment coefficients with respect to α and evaluated for α=0. As customary in aeroelasticity (Salvatori and Borri 2007), the following approximation of indicial functions via exponential filters is adopted in Eq. (4):

$$\Phi_{jk}(t) = 1 - \sum_{i=1}^{N_{jk}} a_i^{jk} \exp\left(-b_i^{jk}\frac{2U}{B}t\right), \quad j = L,M \quad k = h,\alpha \tag{5}$$

The dimensionless parameters a_i^{jk} and b_i^{jk}, which appear in Eq. (5), can be identified by means of an optimization procedure. In particular, the parameters a_i^{Lh} and b_i^{Lh} can be identified, for instance, by minimizing the following cost functional E^{Lh} (Costa and Borri 2006):

$$E^{Lh} = \left\| \tilde{H}_1^* - H_1^* \right\| + \left\| \tilde{H}_4^* - H_4^* \right\| \tag{6}$$

where H_1^*, H_4^* denote measured aeroelastic derivatives while $\tilde{H}_1^*$, $\tilde{H}_4^*$ denote calculated aeroelastic derivatives using the identified parameters a_i^{hk} and b_i^{hk}. Indeed, relations between indicial functions and aeroelastic derivatives can be derived as described in reference (Costa and Borri 2006). Similar expressions to Eq. (6) can also be written for the remaining pairs of aeroelastic derivatives. Clearly, the number of exponential groups N_{jk} in Eq. (5) accounts for the desired level of accuracy in the identification of indicial functions. Indeed, as N_{jk} is increased, a better fitting of the aeroelastic derivatives and, consequently, a more accurate calculation of the critical flutter solution are achieved (Tiffany and Adams 1988).

3. Aeroelastic stability analysis of deck-MTMD system

The aeroelastic stability analysis of the deck-MTMD system can be reduced to a straightforward eigenvalue problem by rewriting the equations of motion in the form of a first order autonomous system. This approach results rather easy in the case of the thin airfoil in which the equations of motion of the uncontrolled system can be reduced in a 6-dimensional state space form, by adding two additional variables based on Wagner's function (Coller and Chamara 2004). For a general bluff deck section, an additional state variable for each exponential filter in Eq. (5) can be introduced as:

$$
\begin{aligned}
w_i^{Lh} &= \int_0^t \frac{b_i^{Lh} a_i^{Lh}}{b} \exp\left(-b_i^{Lh}\frac{U}{b}(t-\tau)\right)\dot{h}(\tau)d\tau \quad i = 1,2,...,N_{Lh} \\
w_i^{L\alpha} &= \int_0^t \frac{b_i^{L\alpha} a_i^{L\alpha} U}{b} \exp\left(-b_i^{L\alpha}\frac{U}{b}(t-\tau)\right)\alpha(\tau)d\tau \quad i = 1,2,...,N_{L\alpha} \\
w_i^{Mh} &= \int_0^t \frac{b_i^{Mh} a_i^{Mh}}{b} \exp\left(-b_i^{Mh}\frac{U}{b}(t-\tau)\right)\dot{h}(\tau)d\tau \quad i = 1,2,...,N_{Mh} \\
w_i^{M\alpha} &= \int_0^t \frac{b_i^{M\alpha} a_i^{M\alpha} U}{b} \exp\left(-b_i^{M\alpha}\frac{U}{b}(t-\tau)\right)\alpha(\tau)d\tau \quad i = 1,2,...,N_{M\alpha}
\end{aligned}
\tag{7}
$$

In the case, for instance, in which one single exponential group is considered for each indicial function, the superscripts in the left-hand side of Eq. (7) can be omitted and the additional variables can simply be indicated as:

$$
\begin{aligned}
w_1 &= w_1^{Lh} \\
w_2 &= w_1^{L\alpha} \\
w_3 &= w_1^{Mh} \\
w_4 &= w_1^{M\alpha}
\end{aligned}
\tag{8}
$$

For reasons that will be discussed in Section 5, this case will be considered in the following developments of the present study. Substituting Eq. (5) into Eq. (4) and using the Eqs. (7) and (8), self-excited lift L and pitching moment M can be rewritten as:

$$
\begin{aligned}
L &= \frac{1}{2}\rho U^2 B C_L'\left((1-a_1^{Lh})\frac{\dot{h}}{U} + (1-a_1^{L\alpha})\alpha + w_1 + w_2\right) \\
L &= \frac{1}{2}\rho U^2 B^2 C_M'\left((1-a_1^{Mh})\frac{\dot{h}}{U} + (1-a_1^{M\alpha})\alpha + w_3 + w_4\right)
\end{aligned}
\tag{9}
$$

Moreover, differentiating Eq. (7) with respect to time t, the following first order differential equations are easily obtained:

$$
\begin{aligned}
\dot{w}_1 &= \frac{b_1^{Lh} a_1^{Lh}}{b}\dot{h} - w_1 \\
\dot{w}_2 &= \frac{b_1^{L\alpha} a_1^{L\alpha} U}{b}\alpha - w_2 \\
\dot{w}_3 &= \frac{b_1^{Mh} a_1^{Mh}}{b}\dot{h} - w_3 \\
\dot{w}_4 &= \frac{b_1^{M\alpha} a_1^{M\alpha} U}{b}\alpha - w_4
\end{aligned}
\tag{10}
$$

Substituting Eq. (9) into Eq. (3) and including Eq. (10) the problem can be reduced in state space

form as:

$$\dot{X} = A(U) \cdot X \tag{11}$$

where A is a real 12×12 matrix depending on the wind velocity U and the state vector X is defined as:

$$X = (\zeta, \dot{\zeta}, \gamma, \dot{\gamma}, \tilde{h}_{T1}, \dot{\tilde{h}}_{T1}, \tilde{\alpha}_{T1}, \dot{\tilde{\alpha}}_{T1}, w_1, w_2, w_3, w_4)^T \tag{12}$$

The extension of the above described procedure to consider a MTMD composed by n TMDs and to use an arbitrary number $k = N_{Lh} + N_{L\alpha} + N_{Mh} + N_{M\alpha}$ of exponential groups is straightforward. Eventually, a system of ordinary differential equations (ODEs) of the form of Eq. (11) is obtained, in which the state vector is defined as:

$$\begin{aligned} X = (\zeta, \dot{\zeta}, \gamma, \dot{\gamma}, \tilde{h}_{T1}, \dot{\tilde{h}}_{T1}, \tilde{\alpha}_{T1}, \dot{\tilde{\alpha}}_{T1}, \ldots, \tilde{h}_{Tn}, \dot{\tilde{h}}_{Tn}, \tilde{\alpha}_{Tn}, \dot{\tilde{\alpha}}_{Tn}, w_1^{Lh}, \ldots, w_{N_{Lh}}^{Lh}, w_1^{L\alpha}, \ldots, \\ w_{N_{L\alpha}}^{L\alpha}, w_i^{Mh}, \ldots, w_{N_{Mh}}^{Mh}, w_i^{M\alpha}, \ldots, w_{N_{M\alpha}}^{M\alpha})^T \end{aligned} \tag{13}$$

and A results to be a $\underline{n}$×$\underline{n}$ matrix, with $\underline{n}$=4(n+1)+k.

Looking at Eqs. (12) and (13) it is clear that considering a general bluff section reflects on a larger dimensional problem with respect to the airfoil case. Indeed, the number of state variables in Eq. (12) grows as the number of exponential filters adopted to approximate indicial functions and the minimal dimension of the system, in the uncontrolled case, is equal to 8.

After rewriting the equations of motion in first order form (Eq. (11)), the aeroelastic stability analysis of the deck-MTMD system can simply be performed by calculating the eigenvalues of matrix A. The flutter instability is encountered when a pair of complex conjugate eigenvalues have zero real parts (Hopf bifurcation point). The minimal velocity U_{crit} at which this condition is satisfied is the critical velocity of the system, while the imaginary part ω_{crit} of the critical eigenvalue represents the circular frequency of the motion at criticality.

4. Optimal robust design of MTMDs

4.1. General design methodology

Before presenting a numerical example in Section 5, a design methodology for MTMDs is presented here, with a particular attention to the mitigation of mistuning effects.

As initial design guess, the classic Den Hartog's rules (Den Hartog 1956) can be adopted to calculate frequency tuning and damping parameter for the STMD (ε=0). Particularly, the uncontrolled critical circular frequency can be utilized as the target frequency and the damping ratio of the device can be initially fixed to the Den Hartog's optimum ξ^{opt} calculated with respect to the twist mode. The adequacy of such rules for tuning STMDs for bridge flutter control is discussed in the design example.

When MTMDs are concerned, the complexity of the system is greatly increased and design formulas might be substituted by the solution of suitable optimization problems (Kwon and Park 2004). To this end, the following parameter η is here considered as the evaluation criterion of control effectiveness:

$$\eta = \frac{U_{crit}^{MTMD} - U_{crit}}{U_{crit}} \tag{14}$$

where U_{crit}^{MTMD} denotes the critical velocity of the deck-MTMD system, while U_{crit} is the uncontrolled one. For a general IMTMD, the optimal design problem can be written as the maximization of η in the space of the design parameters. A similar approach does not however consider the aerodynamic and mechanical uncertainties that characterize the problem, whose main consequence is to cause frequency mistuning that may severely impair the overall effectiveness of the control device.

In order to obtain a robust design, the uncertainties that affect the system should be modeled and incorporated in the optimal design problem. To this regards, Kwon and Park (2004) introduced the concept of minimum flutter velocity U_{crit}^{min}, which is defined as the minimum value of the critical velocity in the space of perturbed aeroelastic derivatives. The optimal design problem of the IMTMD was then stated by the authors as the maximization of U_{crit}^{min}.

From a probabilistic point of view, aerodynamic and mechanical uncertainties might be also taken into account by modeling the critical velocity as a random variable depending on uncertain aeroelastic derivatives and uncertain structural parameters. In the spirit of the well-established "level 1" reliability analysis, the safety requirement of the structure is then satisfied when a characteristic value $U_{crit,k}^{MTMD}$ of the critical velocity of the bridge-MTMD system is sufficiently large. Thus, the control effectiveness can be expressed by means of the evaluation criterion η_k which can be defined as:

$$\eta_k = \frac{U_{crit,k}^{MTMD} - U_{crit,k}}{U_{crit,k}} \tag{15}$$

where $U_{crit,k}$ denotes the characteristic value of the critical velocity of the uncontrolled bridge. The optimal robust design problem of the IMTMD can then be written as:

$$\begin{aligned} &\text{maximize}[\eta_k] \\ &n, \underline{x}, \underline{\omega}_T, \underline{\xi}_T, \underline{m}_T \\ &x_{min} \le x_i \le x_{max} \quad \xi_{T,min} \le \xi_{Ti} \le \xi_{T,max} \quad \omega_{T,min} \le \omega_{Ti} \le \omega_{T,max} \quad \sum_{i=1}^{n} m_{Ti} \le m_{T,max} \end{aligned} \tag{16}$$

where the following vectors containing the design parameters of the single TMDs composing the IMTMD have been introduced:

$$\begin{aligned} \underline{x} &= [x_1, x_2, \ldots, x_n]^T \quad \underline{\omega}_T = [\omega_{T1}, \omega_{T2}, \ldots, \omega_{Tn}]^T \\ \underline{\xi}_T &= [\xi_{T1}, \xi_{T2}, \ldots, \xi_{Tn}]^T \quad \underline{m}_T = [m_{T1}, m_{T2}, \ldots, m_{Tn}]^T \end{aligned} \tag{17}$$

while x_{min}, x_{max}, $\xi_{T,min}$, $\xi_{T,max}$, $\omega_{T,min}$, $\omega_{T,max}$ and $m_{T,max}$ are design constraints. The problem stated in Eq. (16) can be regarded as a general probabilistic framework for the optimal robust design of IMTMDs against bridge flutter. Finding the solution for such a problem might reveal however computationally expensive, as it would require to perform MonteCarlo simulations at every optimization step. Details on possible solution strategies for a similar problem, based on evolutionary algorithms, can be found in (Kwon and Park 2004).

4.2. Simplified design approach

The aim of the present investigation is to outline the mechanical mechanisms that regulate sensitivity against mistuning effects. To this end, a simplified version of the problem stated in Eq. (16) is sought to be adopted in the design example presented in Section 5.

First of all, for the sake of simplicity, the number of freely varying parameters is reduced by introducing the following expression of the natural frequency of the *i*-th TMD composing the MTMD:

$$\omega_{Ti} = \omega_T\left(1 + \varepsilon - \frac{2\varepsilon \cdot (i-1)}{(n-1)}\right), \quad i = 1,2,...,n \tag{18}$$

The detuning parameter ε=0-1 is utilized in Eq. (18) to define the frequency bandwidth of the MTMD, which is equal to $[\omega_T(1-\varepsilon),\omega_T(1+\varepsilon)]$. Thus, according to Eq. (18), ω_T represents the central frequency tuning of the MTMD. The assembled TMDs are also assumed to be placed at the mid-span of the bridge, which is likely the best position for controlling the coupled flutter instability of the first in-plane symmetric and the first torsional symmetric modes, and their damping ratios are assumed to be equal to the same value ξ_T.

As already mentioned, including uncertainties in the analysis would strongly increase the computational effort. However, if the sensitivity of the system to a perturbation $\Delta\omega_T$ of ω_T is reduced, the capability of the system to counteract possible frequency mistuning is certainly improved and η_k is increased. To this end, the following two requirements should be met:

- the η vs ω_T curves should be "wide" around the optimal tuning $\omega_T = \omega_{T,opt}$;
- the variation of η should not be sensitive to the sign of $\Delta\omega_T$.

The former condition stated above is quite trivial, while the latter entails that the η vs ω_T curves should be almost symmetric around the optimal tuning. As it is well-known (Abe and Fujino 1994), the former condition can be satisfied by slightly enlarging the detuning parameter ε in Eq. (18). Concerning the latter condition, as it will be shown in the design example discussed in Section 5, the symmetry of the η vs ω_T curves around the optimal tuning is essentially dictated by the position, in the complex plane, of the critical eigenvalue at the perfectly tuned condition. For the reasons that will be better explained in Section 5, this fundamental requirement can be met by considering an irregular mass distribution of the TMDs. Here, the following rule is considered, which preserves the total amount of mass of the regular MTMD:

$$\psi_i = \frac{\psi}{n} \cdot \delta + \psi \cdot (1-\delta) \cdot \frac{(i-1)}{\sum_{k=1}^{n-1} k}, \quad i = 1,2,...,n \quad 0 \le \delta \le 1 \tag{19}$$

where ψ indicates the total generalized vertical mass ratio of the MTMD. From Eq. (19) it is clear that δ indicates the quote of the total mass which is equally distributed among the TMDs, while (1-δ) indicates the quote of the total mass which is linearly distributed among them. Obviously, the regular MTMD can be interpreted as the considered IMTMD with δ=1.

Now, on the basis of the previous observations and by exploiting the Eqs. (18) and (19), Eq. (16) can be simplified into a suboptimal design problem that still accounts for mistuning effects while relying on the deterministic objective function defined in Eq. (14). The proposed approach is based on the definition of a minimum required control effectiveness $\overline{\eta}$ that must be guaranteed for a

given maximum perturbation amplitude $\Delta\omega_T$ of the frequency tuning. This last is obviously related to the severity of possible frequency mistuning and, consequently, to the level of uncertainties. A feasible approach is to define $\Delta\omega_T$ as a characteristic value of the variation of the uncontrolled critical circular frequency with respect to the nominal case. Once the value of $\Delta\omega_T$ is chosen, an optimal solution is searched under the constraint that $\eta > \overline{\eta}$ for ω_T varying in the interval $[\omega_{T,opt} - \Delta\omega_T, \omega_{T,opt} + \Delta\omega_T]$, $\omega_{T,opt}$, being the optimal tuning. The final design problem can thus be written with the following mathematical structure:

$$\begin{aligned} &\text{maximize}[\eta] \text{ with } \eta > \overline{\eta} \text{ for } \omega_{T,opt} - \Delta\omega_T \le \omega_T \le \omega_{T,opt} + \Delta\omega_T \\ &n, \omega_T, \xi_T, \varepsilon, \delta \\ &\xi_{T,min} \le \xi_T \le \xi_{T,max} \omega_{T,min} \le \omega_T \le \omega_{T,max} \quad 0 \le \varepsilon \le 1 \quad 0 \le \delta \le 1 \end{aligned} \tag{20}$$

By operating in the above described way, it is expected that η_k corresponding to the final design is greater than $\overline{\eta}$, because, with a given level of confidence, frequency mistuning is confined in the interval $[\omega_{T,opt} - \Delta\omega_T, \omega_{T,opt} + \Delta\omega_T]$. Clearly, this simplified approach relies on the fundamental hypothesis that, at a first approximation, mistuning can be assimilated to a perturbation of ω_T. Nonetheless, an a posteriori confirmation that $\eta_k > \overline{\eta}$ can easily be obtained through a straightforward MonteCarlo simulation of the control effectiveness of the designed IMTMD, considering all sources of uncertainties involved in the problem.

5. Control effectiveness of multiple tuned mass dampers

5.1. The case study

A case study is considered to investigate the effectiveness of MTMDs for suppressing the onset of the flutter instability of bridge decks. The considered structure is represented by the New Carquinez Bridge (NCB), which is a suspension bridge crossing over the Carquinez Strait in California. The bridge has a main span of 728 m and two lateral spans of 147 m (southern) and 181 m (northern). It is implicit, however, that the results presented in this work do not refer to the real safety and capacity of the structure.

The mechanical and geometric characteristics of the considered model are summarized in Table 1, where m and I are the vertical and rotational masses of the deck per unit length. These properties, along with the structural mode shapes, have been deduced from a finite element model of the bridge updated on the basis of output only system identification results, using on-site recorded structural responses, in a previous work (Ubertini 2008b).

As reported in (Scanlan and Jones 1998), the deck of the NCB exhibited different aeroelastic derivatives in cases the direction of the incident flow was westward or eastward. This circumstance is due to the flow modifications induced by the presence of another bridge, built in 1958, close to the NCB on one side. The aeroelastic stability analysis performed by Scanlan and Jones (1998) through wind tunnel experiments showed that a flutter instability of the NCB occurred at 74 m/s for eastward wind velocity. On the contrary, no aeroelastic instability was detected for westward wind velocity up to 150 m/s and over. Thus, the aeroelastic behavior of the bridge in the former case is considered in this paper.

Indicial functions of the NCB have been here identified from measured aeroelastic derivatives using Eqs. (5) and (6) through an evolutionary algorithm (Ubertini 2008b). Entering in deep details of the identification phase goes beyond the purposes of the present study. However, some preliminary results, which are necessary for choosing the number of exponential filters in Eq. (5), are presented before analyzing the control effectiveness of regular and irregular MTMDs.

In the uncontrolled case, the exact solution of the flutter equations in the frequency domain, calculated through the procedure described in reference (Robertson, *et al.* 2003), leads to the results summarized in Table 2, which well agree with those reported by Scanlan and Jones (1998). The critical condition is also calculated through the time domain approach using indicial functions. The direct eigenvalue problem is solved by adopting increasing numbers of exponential groups for each indicial function in Eq. (5), up to N_{jk} =3. Some relevant results obtained in these cases are also summarized in Table 2, which show that, as expected, the overall accuracy is improved as the number of exponential filters is increased.

The errors in the calculation of U_{crit} and ω_{crit}, when using one single exponential group for each indicial function, result to be equal to 6.2% and 3.9%, respectively. For the purpose of this study,

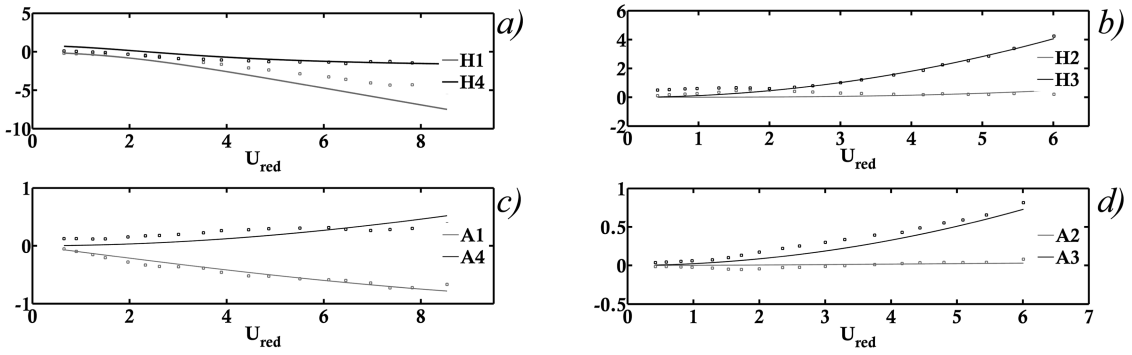

Fig. 2 Fitted (continuous lines) and measured (square points) aeroelastic derivatives of the NCB (1 group for each indicial function)

Table 1 Mechanical characteristics of the model assumed as case study

B (m)	l (m)	ω_h (rad/s)	ω_α (rad/s)	m (kg/m)	I (kg·m^2/m)	ξ_h	ξ_α
27.2	13.6	1.22	2.89	21105	$2.02 \cdot 10^6$	0.03	0.03

Table 2 Results of the aeroelastic stability analysis in the uncontrolled case

Exact solution in the frequency domain					
U_{crit} (m/s)					ω_{crit} (rad/s)
74.1					2.55
Approximate solutions in the time domain					
N_{jk}	N_{MH}	$N_{L\alpha}$	$N_{M\alpha}$	U_{crit} (m/s)	ω_{crit} (rad/s)
1	1	1	1	78.7	2.65
2	2	1	1	74.0	2.67
3	3	3	1	74.8	2.57

which is to outline a general methodology and to apply it to a sample case study, this case is considered here and regarded as "exact" in the numerical calculations presented below. Indeed, along with a good approximation of the critical solution, this choice guarantees a reduced computational effort and a limits the complexity of the problem by minimizing the dimension of the state matrix A. It must be mentioned, however, that more accurate estimations of ω_{crit}, such as the one obtained in the third case reported in Table 2, might be convenient for real design applications. Indeed, errors in the target frequency should be as much smaller as possible than the maximum expected mistuning caused by aerodynamic and mechanical uncertainties.

The comparison between measured and approximated aeroelastic derivatives of the NCB, showing to some extent the quality of the optimization results, is shown in Fig. 2, where U_{red} denotes the reduced velocity (Simiu and Scanlan 1996).

5.2. Design assumptions

In the considered case study, assuming ψ=0.01, corresponding to a total generalized torsional mass ratio ψ_α=0.0193, the following design criteria have been chosen in Eq. (20): perturbation amplitude $\Delta\omega_T = 0.05 \cdot \omega_{T,opt}$ and minimum control effectiveness $\overline{\eta} = 30\%$. Indeed, preliminary calculations have shown that, assuming a coefficient of variation of the aeroelastic derivatives of 15%, which represents a safe estimation of the scatter observed in wind tunnel experiments of the NCB (Caracoglia 2008), reflects on a coefficient of variation of the critical circular frequency that is about 0.3%. Thus, the chosen value of the perturbation amplitude represents a quite safe measure of a possible frequency mistuning, also accounting for mechanical uncertainties and model's errors. Moreover, the maximum control effectiveness that can be achieved through the optimal STMD, in the presented case, is estimated as 45%. Thus, the chosen value of $\overline{\eta}$ represents a reasonable minimum control effectiveness to be required in a "large" frequency bandwidth. Clearly, for a fixed value of the mass ratio, the minimum required control effectiveness $\overline{\eta}$ should be decreased as $\Delta\omega_T$ is increased. On this respect, it is also worth noting that the maximum control effectiveness achievable for a fixed value of the mass ratio strongly depends on the case study and cannot be generalized. Indeed, in the work by Kwon and Park (2004), larger control effectiveness than those obtained here were achieved for another case study by adopting a similar value of the mass ratio. On the other hands, literature works can be found in which the control effectiveness of STMDs with similar mass ratios are either smaller (see for instance, the experimental work by Gu, *et al.* (1998)) or approximately similar (Lin, *et al.* 2000) to the one obtained here.

Regarding the choice of the number n of the assembled TMDs, it is worth noting that, according to Eq. (18), a larger n entails that the TMDs are more closely spaced in terms of frequencies (with the same frequency bandwidth), which is expected to entail beneficial effects on the control effectiveness as the interactions between the TMDs are enhanced. On the other hand, however, as n grows the masses of the single TMDs decrease with the consequence that their control effectiveness diminishes. Clearly, an optimum value of n must be sought, which is expected to depend upon the detuning parameter ε, i.e., on the frequency bandwidth. Here, n=5 has been chosen on the basis of preliminary calculations that are not reported for the sake of brevity.

5.3. Regular MTMD

The first topic under investigation is the effect of the frequency tuning of the MTMD on the

control performance, by considering different values of the detuning parameter ε. To analyze this point, the critical conditions are solved for different values of ω_T and for the following values of the detuning parameter: ε=0 (STMD case), ε=0.05, ε=0.10 and ε=0.15.

The results of the analysis, presented in Fig. 3(a), emphasize that the STMD is the most sensitive to mistuning effects with a peak of control effectiveness η of about 36% for a non-optimum damping ratio. An increment of the detuning parameter (see for instance, the case ε=0.10) guarantees a reduction of the sensitivity to mistuning effects, i.e., the frequency bandwidth of control effectiveness is enlarged, at the expense of reducing the peak of effectiveness at the perfectly tuned condition. Finally, as the detuning parameter reaches relatively large values, the η vs. ω_T curves evidence an overall loss of control effectiveness of the MTMD.

Fig. 3(b) shows the reduced critical circular frequency $K_{crit} = B\omega_{crit}/U_{crit}$ of the system as a function of ω_T. In the STMD case, the optimal tuning may either correspond to a sharp point or even a cusp of the K_{crit} vs. ω_T line, in which K_{crit} attains a global minimum. The effect of an increasing detuning parameter ε is to smoothen this sharp minimum.

The role of the damping ratio ξ_T of the MTMD also deserves some attention. To analyze this point, the critical conditions are solved by varying the ratio ξ_T/ξ^{opt} for the case ω_T=2.46 rad/s, which represents the optimal tuning for ε=0 in Fig. 3(a). The results, presented in Fig. 4(a), emphasize that the optimal damping ratio of the MTMD depends on the detuning parameter ε. Indeed, the optimal

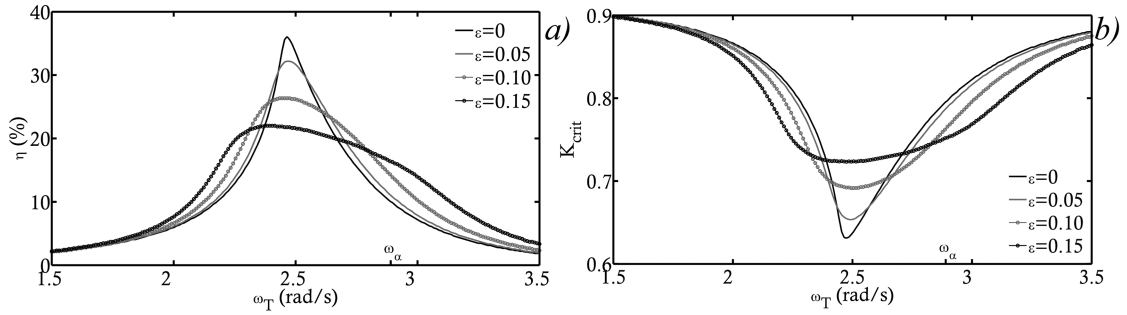

Fig. 3 (a) Control effectiveness of MTMDs by varying the frequency tuning ω_T and the detuning parameter ε and (b) critical circular frequency as a function of ω_T and ε

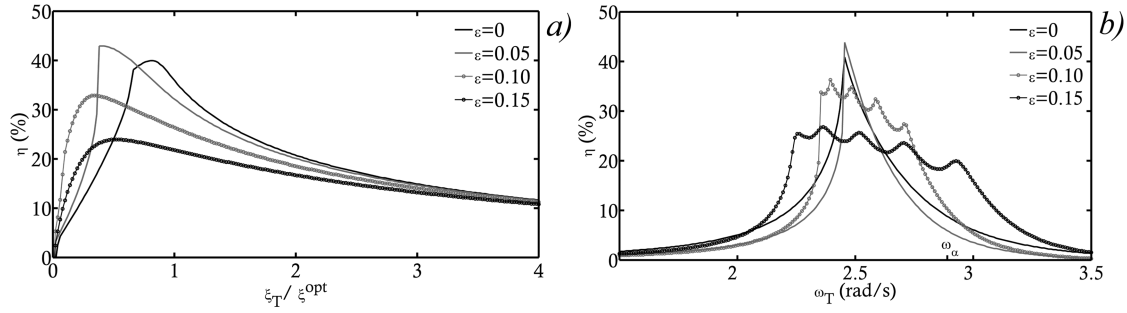

Fig. 4 (a) Control effectiveness of MTMDs by varying the damping ratio and the detuning parameter ε (ξ^{opt} denotes the optimum Den Hartog's value for the twist mode, ω_T=2.46 rad/s) and (b) control effectiveness of MTMDs by varying the frequency tuning ω_T assuming the optimal damping ratios

damping ratio ξ_T of the STMD is roughly equal to $0.80 \cdot \xi^{opt}$, in the cases ε=0.05 and ε=0.10 it is close to $0.38 \cdot \xi^{opt}$ and $0.32 \cdot \xi^{opt}$, respectively, while for ε=0.15 it is slightly larger than $0.5 \cdot \xi^{opt}$. These results suggest that the Den Hartog's rule gives a satisfactory approximation of the optimal damping ratio of the STMD. On the contrary, for ε>0 it becomes a poorer indicator, although it can still be useful for an initial design guess. In particular, the presented results show that as ε is increased the optimal damping ratio initially decreases. Then, when ε becomes relatively large, the assembled TMDs become weakly interacting and the optimal damping ratio tends again to the optimum value of the STMD, with a reduced peak of control effectiveness. It is also worth noting that, in Fig. 4(a), the lines η vs. ξ_T/ξ^{opt} evidence cusps and jumps at certain values of ξ_T/ξ^{opt}. This circumstance entails that, in some cases, a small variation of the damping of the system may reflect on a significant loss of control effectiveness. Thus, damping optimization reveals to be extremely important to fully exploit the control capabilities of the MTMD.

Fig. 4(b) shows the curves of control effectiveness of MTMDs by fixing the damping ratios to their optimal values obtained in Fig. 4(a). First of all, it must be mentioned that the optimal tuning of the STMD reveals to be only about 6% times smaller than the optimal Den Hartog's criterion. This confirms, to some extent, the accuracy of such a tuning rule in the case of STMDs for bridge flutter control. On the contrary, similarly to the damping case, as ε becomes greater than 1, the behavior of the system becomes more complex and such a rule partially loses its effectiveness. It is also important to note that the η vs. ω_T curves in Fig. 4(b) sometimes assume an asymmetric aspect of the "softening-type", which means that the optimal tuning tends to be located on the edge of the optimal region. This circumstance, in the presented case, is particularly evident for ε=0.05 and ε=0.10 and was also observed in other case studies (Ubertini 2008b) that are not reported here for the sake of brevity, as well as in other literature works (Lin, *et al.* 2000). The main consequence of this behavior is that the system might be rather sensitive to a detuning below the optimal value of ω_T. An interpretation of this phenomenon is given below.

The mechanical way in which tuned mass dampers increase the critical velocity is by preventing the eigenvalue of the controlled mode from approaching the instability boundary. This can be achieved by collocating, in the complex plane, the eigenvalues of the tuned mass dampers in the vicinity of the controlled eigenvalue. If the control device is properly designed, instability is finally attained, at a larger critical velocity with respect to the uncontrolled case, by one of the eigenvalues of the tuned mass dampers. It might happen, however, that the critical eigenvalue corresponds to the TMD having the lowest frequency $\omega_T(1-\varepsilon)$ or to that having the largest one $\omega_T(1+\varepsilon)$. In such cases a weak direction for mistuning exists, in which mistuning makes the controlled eigenvalue reach the instability boundary without being strongly interacted. This, indeed, causes a severe loss of control effectiveness. From these considerations it is clear that, when the critical eigenvalue corresponding to the optimal design point is the one having central frequency ω_T, the η vs. ω_T curves are expected to be almost symmetric around the optimal tuning because no weak direction for frequency mistuning exists. As it will be discussed in Section 5.4, this result can be obtained through an irregular mass distribution.

The above described phenomenon can be also illustrated with reference to the case study. To this end, let us consider the optimal tuning of the MTMD with ε=0.10, which is approximately equal to $\omega_{T,opt}$=2.39 rad/s. For such a case, the root locus of the eigenvalues of the system, by increasing the wind velocity up to criticality, is shown in Fig. 5(a), while a detailed view of the path of the critical eigenvalue is shown in Fig. 5(b). A total of 12 pairs of complex conjugate eigenvalues correspond to the DOFs of the structural system. The remaining 4 real eigenvalues, corresponding to the

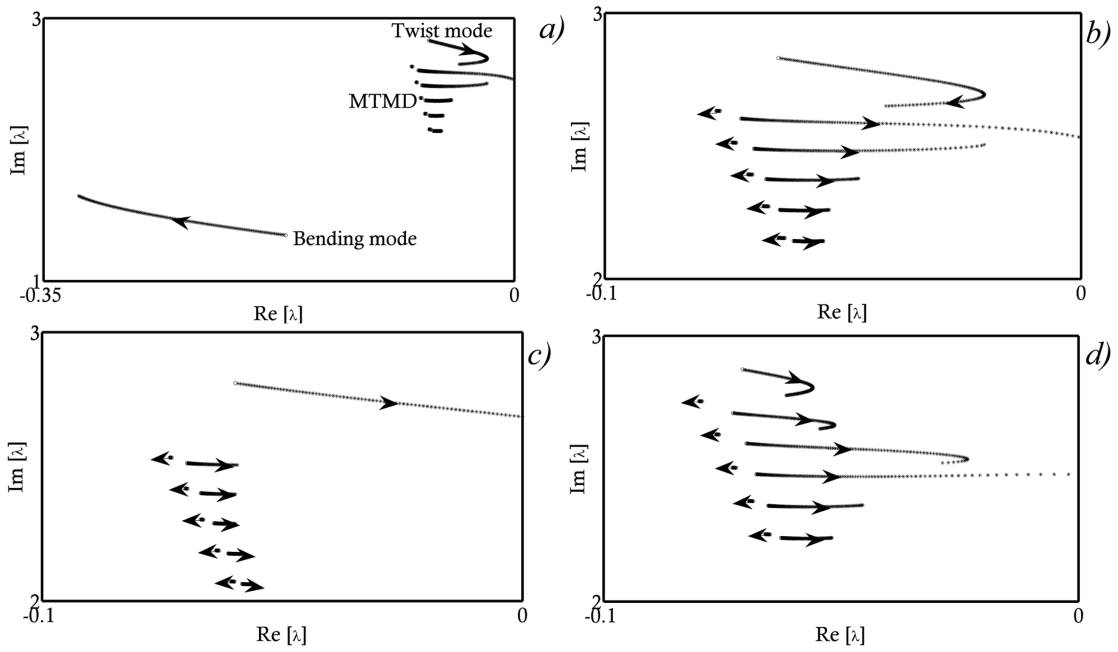

Fig. 5 Root loci of the eigenvalues of the deck-MTMD system by increasing the wind velocity U up to criticality: (a) and (b) ω_T=2.39 rad/s, ε=0.10, ξ_T/ξ^{opt}=0.34, U_{crit}^{MTMD}=107.0 m/s; (c) ω_T=2.30 rad/s, U_{crit}^{MTMD}=88.4 m/s and (d) ω_T=2.50, U_{crit}^{MTMD}=104.9 m/s

additional variables w_i introduced in Eq. (8), complete the total number of eigenvalues of the system. For the sake of clarity, only the upper left quadrant of the complex plane and only the structural eigenvalues are shown in Fig. 5, where λ denotes a general eigenvalue. The indication of the correspondence between eigenvalues and mechanical DOFs is also reported in Fig. 5(a).

The results presented in Figs. 5(a) and 5(b) evidence that the critical eigenvalue is the one corresponding to the twist motion of the TMD having natural frequency $\omega_T(1+\varepsilon)$. By slightly reducing ω_T below the optimum value of 2.39 rad/s, a sudden loss of control effectiveness is observed in Fig. 4(b). In this case, as expected, the critical eigenvalue is the one corresponding to the twist motion of the deck (typical case without control). This phenomenon is evidenced in Fig. 5(c) in which the parameters ε=0.10 and ω_T=2.30 rad/s are adopted in the calculation of the root locus. On the contrary, by increasing ω_T above 2.39 rad/s, instability is attained, one after the other, by the eigenvalues corresponding to the remaining TMDs. As an example, in the case ε=0.10 and ω_T=2.50 rad/s, the critical eigenvalue is the one corresponding to the TMD having the central frequency ω_T (see Fig. 4(d)). Eventually, when ω_T is sufficiently large and the device is essentially ineffective, instability is again attained by the DOF corresponding to the twist motion of the deck.

Before analyzing the behavior of IMTMDs in the next section, it is worth noting that, in all the considered cases, when instability occurs, mechanical and wind couplings make both bending and twist structural modes participate to the critical motion along with the DOFs of the MTMD. As an example, the critical solution in the case ε=0.10 and ω_T=2.39 rad/s, obtained via numerical integration, is shown in Fig. 6. The presented results evidence that the critical condition is, as expected, characterized by a coupled harmonic motion which, in this case, has 12 DOFs.

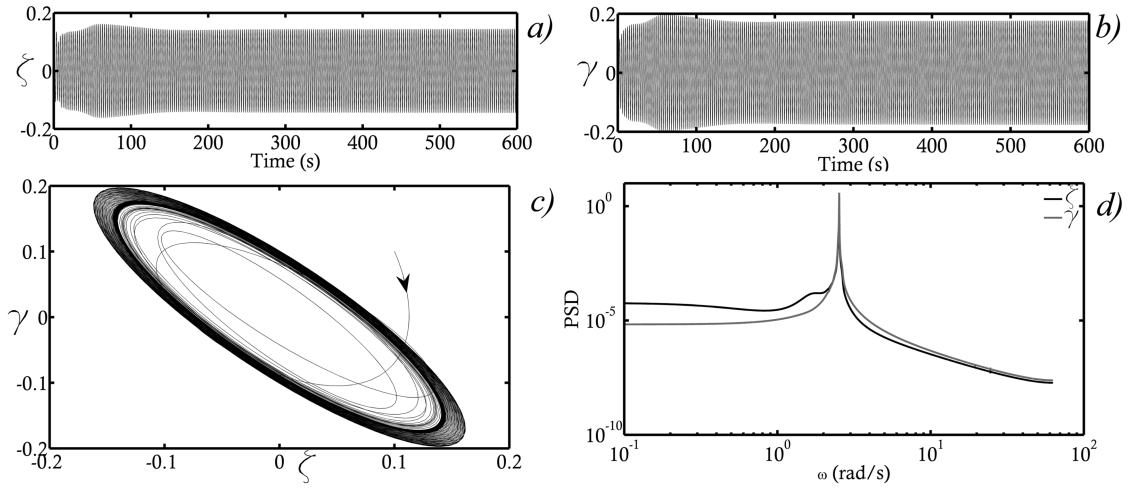

Fig. 6 Critical flutter solution for ω_T=2.39 rad/s, ξ_T/ ξ^{opt}=0.34 and ε=0.10

5.4. Irregular MTMD

The results presented in Section 5.3 have shown that a MTMD composed by n TMDs having equal masses, equal damping coefficients and equally-spaced circular frequencies, guarantees enlarged frequency bandwidth if compared to the STMD. However, the system exhibits non-symmetric η vs. ω_T curves of control effectiveness around the optimal tuning. This last circumstance is especially undesirable in technical applications because it produces a sudden loss of control effectiveness when the device is detuned below the optimal tuning. In order to circumvent this drawback, an IMTMD is considered herein.

As already observed in Section 5.2, the asymmetry of the η vs. ω_T curves occurs when the optimal tuning corresponds to the instability of the TMD with largest frequency $\omega_T(1+\varepsilon)$. On the contrary, the η vs. ω_T curves are expected to be almost symmetric around the optimal tuning when the critical eigenvalue at that point corresponds to the torsional eigenvalue of the TMD having frequency ω_T (central frequency of the MTMD). A possible way for modifying the critical eigenvalue at the perfectly tuned condition is to adopt an IMTMD. This last can be obtained in many ways by destroying the regularity of the MTMD as, for instance, by considering irregular frequency spacing between the TMDs, different damping coefficients and so on. Since the mass ratio is the parameter that mostly affects the interactions between closed eigenvalues, the irregular mass distribution given by Eq. (19) is considered here to mitigate mistuning effects. Preliminary calculations have also shown that such an approach gives better results if compared to an irregular frequency spacing for the purposes of this study. In particular, according to Eq. (19), the IMTMD is obtained from the regular MTMD by increasing the mass ratios of the TMDs with lower frequencies and reducing the mass ratios of the TMDs with larger frequencies. This, indeed, enhances the interactions between the torsional eigenvalue of the structure and the eigenvalues of the MTMD corresponding to lower frequencies, while reducing these interactions with the eigenvalues of the MTMD corresponding to larger frequencies that are, in this way, stabilized. Thus, when an optimum value of δ is found, instability at the perfectly tuned condition is attained by the twist

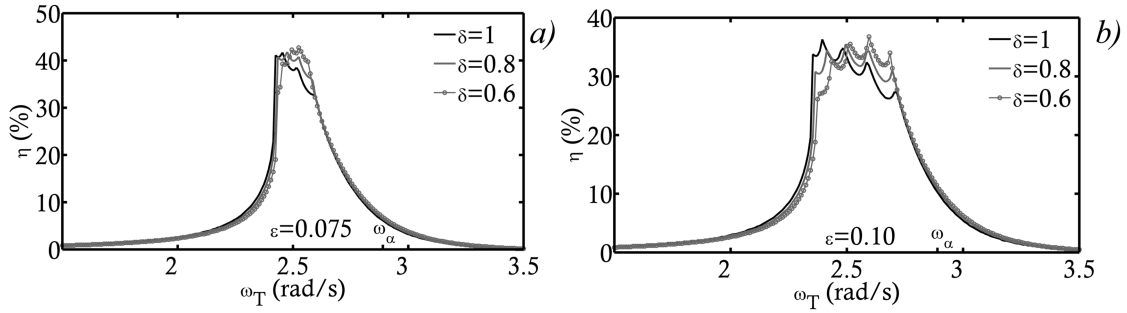

Fig. 7 Improved robustness against mistuning effects through irregular MTMDs

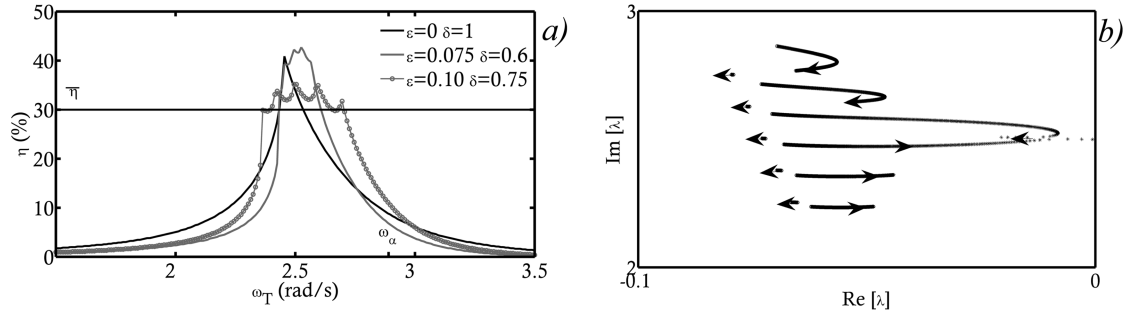

Fig. 8 (a) Comparison between control effectiveness using single TMD and irregular MTMDs and (b) detailed view of the root locus of the eigenvalues of the system for the case ω_T=2.50 rad/s, ε=0.10, δ=0.75

eigenvalue of the TMD having central frequency ω_T.

In order to investigate the effectiveness of the considered IMTMD, the performance index η is calculated by varying the frequency tuning ω_T, for the cases δ=0.80 and δ=0.60, assuming the optimal damping ratio for each case. The results, presented in Fig. 7, confirm that the η vs. ω_T curves of the IMTMD are almost symmetric around the optimal tuning when δ attains an optimum value. Fig. 8(a) shows the comparison between the STMD and two relevant cases of IMTMDs. The presented results clearly outline the benefit obtained by considering IMTMDs instead of the STMD in terms of sensitivity against frequency perturbations. A detailed view of the root locus of the eigenvalues of the IMTMD with ε=0.10 and δ=0.75 at the perfectly tuned condition is reported in Fig. 8(b). The presented results confirm that, in this case, instability is attained by the eigenvalue corresponding to the TMD having central frequency ω_T.

The IMTMD with ε=0.10 and δ=0.75 proves to be a good compromise between control effectiveness and robustness. Indeed, this case is characterized by a rather "large" optimal region where the performance index η is larger than $\overline{\eta}$ (see Fig. 8(a)). Moreover, in such a case the global optimum seems to be located in the middle of such region, thus entailing that global optimization also produces robustness against frequency mistuning in the sense of Eq. (20). The final effort is now to contemporary optimize both ω_T and ξ_T for the case ε=0.10 and δ=0.75. This will allow to find a sort of global optimal solution accounting for both control effectiveness and robustness. To this end, a full domain search of the point of maximum control effectiveness is performed. Figs. 9(a) and 9(b) show the variation of the objective function η with frequency

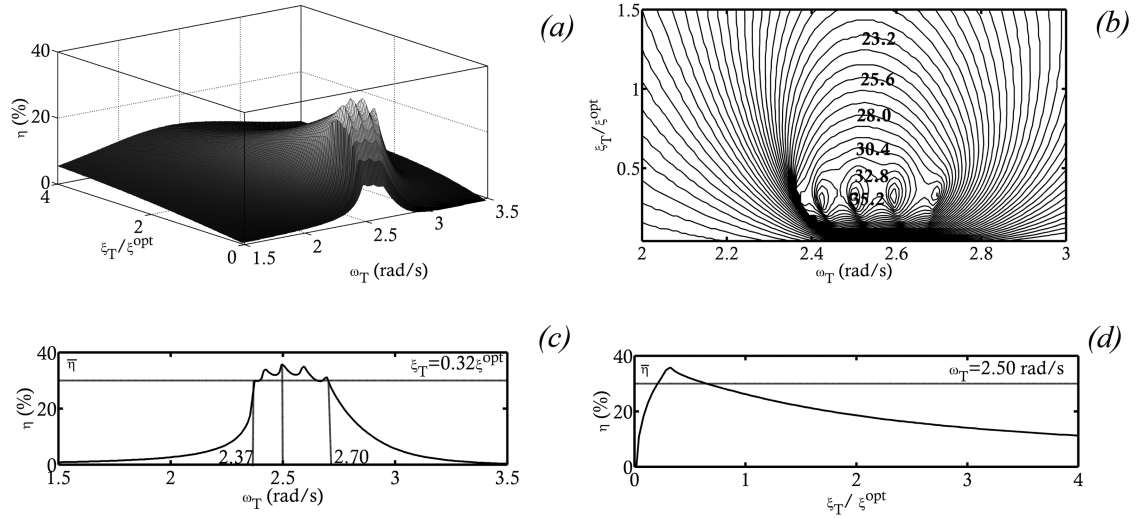

Fig. 9 Control effectiveness of IMTMD (ε=0.10 and δ=0.75) as a function of the damping ratio and of the frequency tuning: (a) tridimensional view of the objective function η, (b) contour plot of the objective function η in the region of the optimal solution (values in percentage), (c) sections of the objective function along the lines corresponding to the optimal damping ratio and (d) the optimal frequency tuning

tuning ω_T and damping ratio ξ_T. The results outline that the objective function has five distinct relative maxima which are related to the presence of the five TMDs. These relative maxima are placed above a wide region of large control effectiveness (see Fig. 9(b)) and are almost aligned along the same value of the damping ratio, which is nearly equal to $0.32 \cdot \xi^{opt}$. The middle peak among the five relative maxima is the global optimum, which corresponds to a performance index of 35.8%. The sections of the objective function along the lines corresponding to the optimal damping ratio and the optimal frequency tuning are also shown in Figs. 9(c) and 9(d). These results confirm that the optimal design point (corresponding to $\omega_{T,opt}$=2.50 *rad/s*) satisfies Eq. (20) with $\overline{\eta}$=30% and $\Delta\omega_T$=$0.05 \cdot \omega_{T,opt}$=0.125 *rad/s*. However, it must be mentioned that the system is sensitive to variations of the damping ratio below the optimal value. This entails that assuming $\xi_T > 0.32\xi^{opt}$ appears to be a safer choice with respect to the design of the IMTMD using the theoretical optimal damping ratio.

6. Conclusions

An investigation on bridge flutter control using regular and irregular MTMDs is presented. The aeroelastic stability analysis is reduced to a direct eigenvalue problem by representing the aeroelastic loads through indicial functions. When bluff deck sections are concerned, integral terms can be eliminated by introducing an additional state variable for each exponential group adopted in the approximation of indicial functions. The eigenvalue problem is thus stated and the stability analysis is straightforward.

A general methodology for the optimal robust design of irregular MTMDs is proposed which is

based on modeling the critic velocity as a random variable and on a probabilistic definition of control effectiveness. The proposed approach relies on a level 1 reliability analysis and it is feasible to incorporate all kind of uncertainties that affect the system. Clearly, the solution of the optimization problem requires Monte Carlo simulations to reliably estimate the objective function, which might call for significant computational efforts that, however, can be easily tackled today with the aid of efficient calculators. However, for the purposes of this study, a simplified version of this design approach is also proposed, which still allows to obtain robust designs against frequency mistuning but it adopts a deterministic measure of control effectiveness without any need of performing Monte Carlo simulations.

A general case study is considered in which the simplified design approach is applied and the control capability of MTMDs is investigated. The results show that the optimal tuning of the STMD corresponds to a sharp minimum of the function representing the critical eigenvalue vs. the frequency tuning. In the case of MTMDs this cusp is smoothened and a larger robustness against frequency mistuning is achieved. Optimization of the damping ratio of the MTMD is also primarily important to achieve optimal control solutions. Within this context, the optimal damping ratio is seen to depend upon the detuning parameter of the MTMD. Namely, the optimum is seen to initially decrease as the detuning parameter increases and to tend again to the optimum of the STMD when the detuning parameter becomes large.

Despite the numerous advantages with respect to STMDs, correctly designed MTMDs may still exhibit a softening-type asymmetry with respect to frequency mistuning. This circumstance may impair the overall control effectiveness of the device in technical situations. After giving an interpretation of this phenomenon, an IMTMD with unequal mass distribution is proposed to circumvent this drawback. The IMTMD is seen able to guarantee a significant robustness against mistuning effects, regardless the direction of the detuning. After finding the parameters of the IMTMD offering the best compromise between control robustness and control effectiveness, the frequency tuning and the damping ratio of the device are finally optimized by means of a full domain search. The results show that the objective function possesses a number of relative maxima which equals the number of small tuned mass dampers assembled in the device. These relative maxima are distributed on a wide flat region and the global optimal solution corresponds to the peak placed in the middle of this region. Thus, the analysis evidences, to some extent, a remarkable control robustness of the device, in the sense of the simplified design approach.

Now, having stated the general design problem and having investigated the relevant aspects of the behavior of IMTMDs for bridge flutter control, future developments of this study must deal with the comparison between the results of the simplified design approach and the solution of the general probabilistic optimization problem, with the final purpose of deriving simple design formulas to be adopted in practical applications.

Acknowledgements

The author wishes to gratefully thank Professor A.L. Materazzi, University of Perugia, Italy, for his precious comments and suggestions about this study.

The author also expresses his gratitude to Professor Raimondo Betti, Columbia University, New York, for providing the essential information about the case study structure.

References

Abe, M. and Fujino, Y. (1994), "Dynamic characterization of multiple tuned mass dampers and some design formulas", *Eartq. Eng. Struct. D.*, **23**, 813-835.
Breccolotti, M., Gusella, V. and Materazzi, A.L. (2007), "Active displacement control of a wind-exposed mast", *Struct. Control Health*, **14**, 556-575.
Caracoglia, L. and Jones, N.P. (2003), "A methodology for the experimental extraction of indicial functions for streamlined and bluff deck sections", *J. Wind Eng. Aerod.*, **91**, 609-36.
Caracoglia, L. (2008), "Influence of uncertainty in selected aerodynamic and structural parameters on the buffeting response of long-span bridges", *J. Wind Eng. Aerod.*, **96**, 327-344.
Casciati, F., Magonette, G. and Marazzi, F. (2007), *Technology of Semiactive Devices and Applications in Vibration Mitigation*, John Wiley & Sons, Chichester.
Chen, X. and Kareem, A. (2003), "Efficacy of tuned mass dampers for bridge flutter control", *J. Struct. Eng.-ASCE*, **129**(10), 1291-1300.
Chen, X., Matsumoto, M. and Kareem, A. (2000a), "Aerodynamic coupling effects on flutter and buffeting of bridges", *J. Eng. Mech.-ASCE*, **126**(1), 17-26.
Chen, X., Matsumoto, M. and Kareem, A. (2000b), "Time domain flutter and buffeting response analysis of bridges", *J. Eng. Mech.-ASCE*, **126**(1), 7-16.
Cluni, F., Gusella, V. and Ubertini, F. (2007), "A parametric investigation of wind-induced cable fatigue", *Eng. Struct.*, **29**(11), 3094-3105.
Coller, B.D. and Chamara, P.A. (2004), "Structural nonlinearities and the nature of the classic flutter instability", *J. Sound Vib.*, **277**, 711-739.
Costa, C. and Borri, C. (2006), "Application of indicial functions in bridge deck aeroelasticity", *J. Wind Eng. Aerod.,* **94**, 859-881.
Den Hartog, J.P. (1956), *Mechanical Vibrations, 4th Edition*, McGraw-Hill, New York.
Faravelli, L., Fuggini, C. and Ubertini, F. (2009), "Toward a hybrid control solution for cable dynamics: theoretical prediction and experimental validation", *Struct. Control Health*, DOI: 10.1002/stc.313
Faravelli, L. and Ubertini, F. (2009), "Nonlinear state observation for cable dynamics", *J. Vib. Control*, **15**, 1049-1077.
Gu, M., Chang, C.C., Wu, W. and Xiang, H.F. (1998), "Increase of critical flutter wind speed of long-span bridges using tuned mass dampers", *J. Wind Eng. Aerod.,* **74**, 111-123.
Gusella, V. and Materazzi, A.L. (2000), "Non-Gaussian along-wind response analysis in time and frequency domains", *Eng. Struct.*, **22**, 49-57.
Kareem, A. and Kline, S. (1995), "Performance of multiple mass dampers under random loading", *J. Struct. Eng.-ASCE*, **121**, 348-361.
Kwon, S.D. (2002), "Discussion on control of flutter of suspension bridge deck using TMD", *Wind Struct.*, **5**, 563-567.
Kwon, S.D. and Chang, S.P. (2000), "Suppression of flutter and gust response of bridges using actively controlled edge surfaces", *J. Wind Eng. Aerod.*, **88**(2-3), 263-281.
Kwon, S.D. and Park, K.S. (2004), "Suppression of bridge flutter using tuned mass dampers based on robust performance design", *J. Wind Eng. Aerod.*, **92**(11), 919-934.
Lazzari, M., Vitaliani, R.V. and Saetta, A. (2004), "Aeroelastic forces and dynamic response of long-span bridges", *Int. J. Numer. Meth. Eng.*, **60**, 1011-1048.
Lin, Y.Y., Cheng, C.M. and Lee, C.H. (1999), "Multiple tuned mass dampers for controlling coupled buffeting and flutter of long-span bridges", *Wind Struct.*, **2**(4), 267-284.
Lin, Y.Y., Cheng, C.M. and Lee, C.H. (2000), "A tuned mass damper for suppressing the coupled flexural and torsional buffeting response of long-span bridges", *Eng. Struct.*, **22**, 1195-1204.
Piccardo, G. (1993), "A methodology for the study of coupled aeroelastic phenomena", *J. Wind Eng. Aerod.*, **48**(2-3), 241-252.
Pourzeynali, S. and Datta, T.K. (2002), "Control of flutter of suspension bridge deck using TMD", *Wind Struct.,* **5**, 407-422.
Preidikman, S. and Mook, D.T. (1997), "A new method for actively suppressing flutter of suspension bridges", *J.*

Wind Eng. Aerod., **69-71**, 955-974.
Robertson, I., Sherwin, S.J. and Bearman, P.W. (2003), "Flutter instability prediction techniques for bridge deck sections", *Int. J. Numer. Meth. Fl.*, **43**, 1239-1256.
Salvatori, L. and Borri, C. (2007), "Frequency- and time-domain methods for the numerical modeling of full-bridge aeroelasticity", *Comput. Struct.,* **85**, 675-687.
Scanlan, R.H., Béliveau, J.G. and Budlong, K. (1974), "Indicial aerodynamics functions for bridge decks", *J. Eng. Mech.-ASCE*, **100**, 657-72.
Scanlan, R.H. and Jones, N.P. (1998), *Wind Response Study Carquinez Strait Suspended Span*, Report for West Wind Laboratory, Inc. and OPAC Consulting Engineers.
Simiu, E. and Scanlan, R.H. (1996), *Wind Effects on Structures*, third ed., John Wiley and Sons, New York.
Soong, TT. (1991), *Active Structural Control: Theory and Practice*, Longman Scientific & Technical, England.
Tiffany, S.H. and Adams, W.M. (1988), *Nonlinear Programming Extensions to Rational Function Approximation Methods for Unsteady Aerodynamic Forces*, NASA TP-2776.
Tubino, F. and Solari, G. (2007), "Gust buffeting of long span bridges: Double Modal Transformation and effective turbulence", *Eng. Struct.,* **29**(8), 1698-1707.
Ubertini, F. (2008a), "Active feedback control for cable vibrations", *Smart Struct. Syst.,* **4**(4), 407-428.
Ubertini, F. (2008b), *Wind effects on bridges: response, stability and control*, PhD Dissertation, University of Pavia, Italy.

CC

Notation

The following notation is used in this article:

U	: mean wind velocity;
t	: time;
x	: longitudinal axis of the bridge;
$L(x)$, $M(x)$	: lift and pitching moments per unit length;
n	: number of TMDs of the MTMD system;
$h(x,t)$, $\alpha(x,t)$	: degrees of freedom of the deck;
x_i	: position of i-th TMD along the longitudinal axis of the bridge;
h_{Ti}, α_{Ti}	: degrees of freedom of the i-th TMD;
m_{Ti}, I_{Ti}	: mass and mass moment of inertia of the i-th TMD;
k_{Ti}, c_{Ti}	: vertical stiffness and damping coefficients of the i-th TMD;
B, l	: reference width of the deck and half brace of the TMDs;
b	: half chord of the deck;
ξ_{Ti}, $\xi_{T\alpha i}$, ω_{Ti}, $\omega_{T\alpha i}$	: damping ratios and circular frequencies of the i-th TMD;
φ_h, φ_α	: structural mode shapes;
ζ, γ	: modal amplitudes;
ψ_i, $\psi_{\alpha i}$	: generalized mass ratios of the the i-th TMD;
$\tilde{m}$, I	: generalized modal inertias;
$\tilde{h}_{T1}$, $\tilde{\alpha}_{T1}$	: generalized coordinates of TMD number 1;
ξ_h, ξ_α, ω_h, ω_α	: structural modal damping ratios and circular frequencies;
ϕ_{Lh}, $\phi_{L\alpha}$, ϕ_{Mh}, $\phi_{M\alpha}$	: aerodynamic indicial functions;
τ	: integration variable;
ρ	: air density;

C'_L, C'_M : dynamic derivatives of lift and moment coefficients;
N_{Lh}, $N_{L\alpha}$, N_{Mh}, $N_{M\alpha}$: number of exponential filters for indicial functions approximation;

a_i^{Lh}, $a_i^{L\alpha}$, a_i^{Mh}, $a_i^{M\alpha}$
b_i^{Lh}, $b_i^{L\alpha}$, b_i^{Mh}, $b_i^{M\alpha}$: dimensionless parameters for indicial functions approximation;

E^{Lh} : cost function for indicial functions approximation;

H_1^*, H_2^*, H_3^*, H_4^*
A_1^*, A_2^*, A_3^*, A_4^* : measured aeroelastic derivatives;

$\tilde{H}_1^*$, $\tilde{H}_4^*$: approximated aeroelastic derivatives;
U_{red}, K_{crit} : reduced wind velocity and reduced critical frequency;
w_i^{Lh}, $w_i^{L\alpha}$, w_i^{Mh}, $w_i^{M\alpha}$: additional aerodynamic variables;
X : state vector;
A : first order system matrix;
k : total number of additional aerodynamic variables;
$\underline{n}$: first order system dimension;
U_{crit}, U_{crit}^{MTMD} : uncontrolled and controlled critical velocities;
ω_{crit} : critical eigenvalue;
U_{crit}^{min}, $U_{crit,k}$, U_{crit}^{MTMD} : minimum and characteristic flutter velocities;
η, η_k : evaluation criteria of control effectiveness;

$x_{\min}$, $x_{\max}$, $\xi_{T,\min}$, $\xi_{T,\max}$
$\omega_{T,\min}$, $\omega_{T,\max}$, $m_{T,\max}$: design constraints;

$\underline{x}$, $\underline{\omega_T}$, $\underline{\xi}_T$, $\underline{m_T}$: vectors of design parameters;
ε : detuning parameter;
ω_T : central tuning of the MTMD;
ξ_T : damping ratio of the MTMD;
$\omega_{T,opt}$: optimal tuning;
$\Delta\omega_T$: frequency tuning perturbation;
δ : mass distribution parameter;
ψ, ψ_α : total generalized mass ratios of the MTMD;
$\overline{\eta}$: minimum required control effectiveness;
m, I : mass and mass moment of inertia of the deck per unit length;
ξ^{opt} : optimum Den Hartog's damping ratio;
λ : system eigenvalue.